Soot filtration modeling and simulation in diesel particulate filter

M. Azimian, J. Becker, L. Cheng, A. Wiegmann

Math2Market GmbH, Kaiserslautern, Germany
www.math2market.de , E-Mail: info@math2market.de

In diesel and gasoline engines, it becomes increasingly important to filter soot emissions from the exhaust. Soot emissions can be reduced by forcing the soot particles to be trapped physically through an installed diesel particulate filter (DPF). The DPF is one of the most essential after-treatment devices invented to reduce particulate matter from diesel engines discharge. For optimal protection of environment, the international emission standards become stricter and mandatory for more countries.

The goal of this study was to use computer simulations (GeoDict®) to design a better DPF with lower pressure drop, higher filter efficiency and longer life time. The key parameter that governs the DPF performance is the ceramic filter media. Therefore, the simulation steps contain modeling the ceramic filter media, simulating the air flow through the filter media, simulating the transport and deposition of soot particles, the conversion of deposited particles into a porous media, determining the soot layer packing density and the soot layer's viscous flow resistivity. The simulations provide all the details on deposition location and pressure drop over time.

Soot particles to be filtered are much smaller than the computational grid size. Therefore, when soot particles deposit, they do not fully fill the computational cell, but rather form a permeable media inside and on top of the ceramic filter. The solver allows to control how much a cell can get filled, and how much resistivity to the flow the cell will have, depending on the degree of filling. Sub-voxel-sized soot particles form a filter cake which is modeled as porous media with locally varying permeability. These soot particles do most of the work to filter more particles.

The simulation results show that initially a fast increase in pressure drop occurs during the depth filtration regime. Afterwards, it follows with a long, slower pressure drop increase during the cake filtration regime. The simulation results agree very well with the experimental data provided by Fraunhofer IKTS [1, 2]. Modifications were carried out to shorten the depth phase and to reduce the pressure drop during cake phase. This work confirms a key step in virtual material design. The outcome of the simulation studies led to a granted patent for the particulate filter [3].

Keywords: Soot filtration, multi-scale, simulation, modelling, GeoDict

1. Introduction

The goal of this work is to use computer simulations to find a diesel particulate filter with better filtration properties, i.e. lower pressure drop, higher efficiency, and longer life-time. Along the way towards this goal, the ceramic filter media was identified as one of the key ingredients that govern the DPF performance. In this work, we demonstrate that an improved ceramic filer media can be predicted by simulations. Step by step method of the simulation such as the ceramic media modeling, computation of the air flow, tracking the particles, depositing the particles and converting them to a porous media were established in our previous work [1].

To simulate the life-time soot filtration in ceramic filter media (Figure 1), a DPF micro-structure is firstly modeled. Afterwards, flow field is computed by solving the Navier-Stokes-Brinkman equations. The soot particles are released in the air flow and the movements of the particles are tracked. Due to different mechanisms of filtration, some of the particles are captured and deposited on the solid surfaces of the filter medium. When the volume of the deposited particles grows, the flow field is changed due to the resistance induced by the deposited particles. Therefore, the flow field must be re-computed. New particles are then tracked in the updated flow field through the following batches.

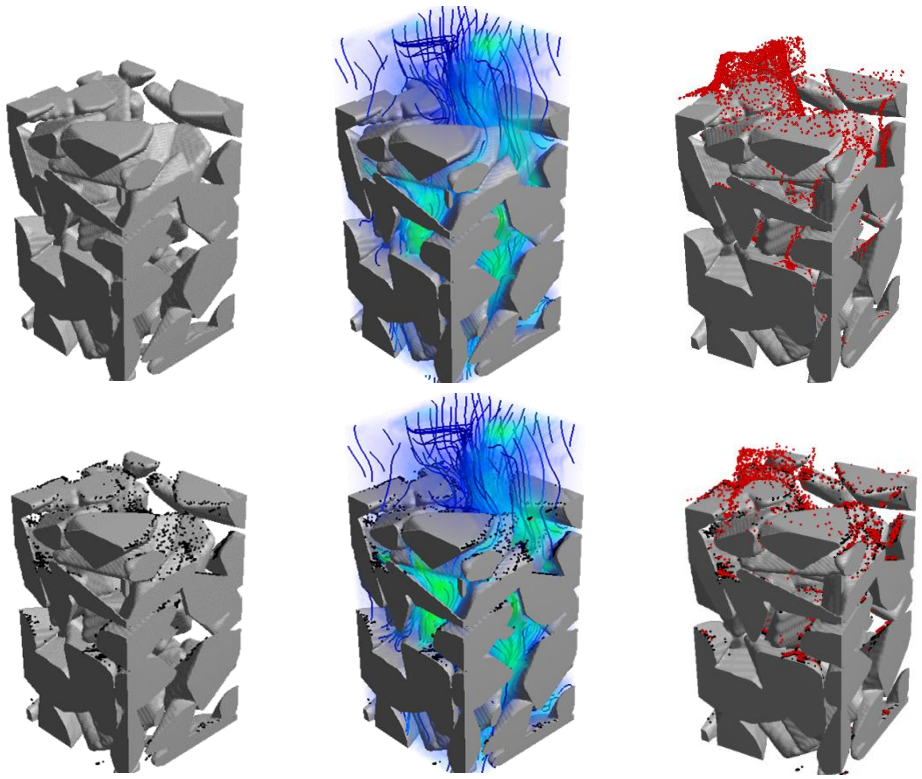

Figure 1: Simulation steps for life-time soot filtration in a ceramic structure: red particles (active), black particles (deposited).

2. Structure generation

The generation of sintered structures comprises two steps: first, the stochastic object generator is used to create ellipsoids, cylinders and other basic geometrical shapes.

In many applications this is done iteratively, e.g. large ellipsoids are generated which represent large pores, then, into the complement of the large ellipsoids smaller ellipsoids are generated which represent the initial grains of the sintered structure. At this stage, it is necessary to check the shape and size distribution of the real sinter grains and try to match these distributions. During the second step, morphological operations [4] are applied to generate the sinter necks. Iteratively using the operations dilatation and erosion creates exactly the intended connectivity.

Quality measures are needed for virtual structures which are intended to reproduce existing media. 2D SEM (Scanning Electron Microscope) images or 3D tomography data of a real sample can be used to compute and compare various geometrical properties like porosity, cord length distribution, pore size distribution, specific surface area, anisotropies, etc. with the GeoDict software package [5]. Figure 2 shows the comparisons between 2D SEM images of three different real ceramic materials and 2D cross section images of the corresponding 3D reconstructions.

In industry, permeability tests of porous samples are standard. Moreover, flow simulations in typical porous media regimes, i.e. slow flow regimes are very reliable. Hence, measured and computed flow properties can be compared quite safely and provide meaningful results. The porosities and permeabilities for different types of ceramic materials are measured and compared with the computed porosities and permeabilities of the corresponding modeled ceramic materials (Figure 3). Reasonable agreements are found comparing the SEM images and the constructed models [7].

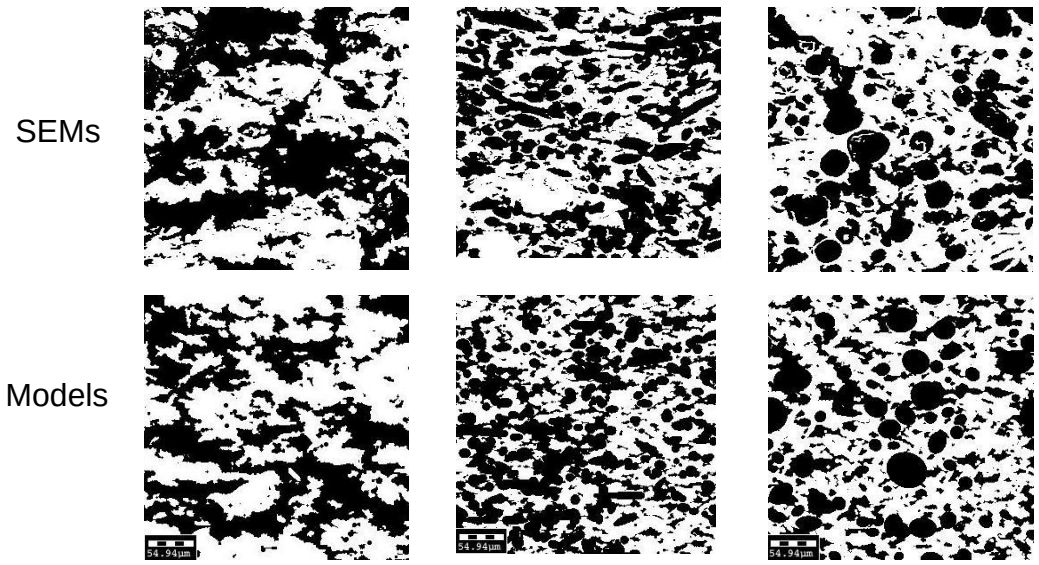

Figure 2: 2D SEM images of real materials and 2D cross section images of the corresponding 3D reconstruction [7]

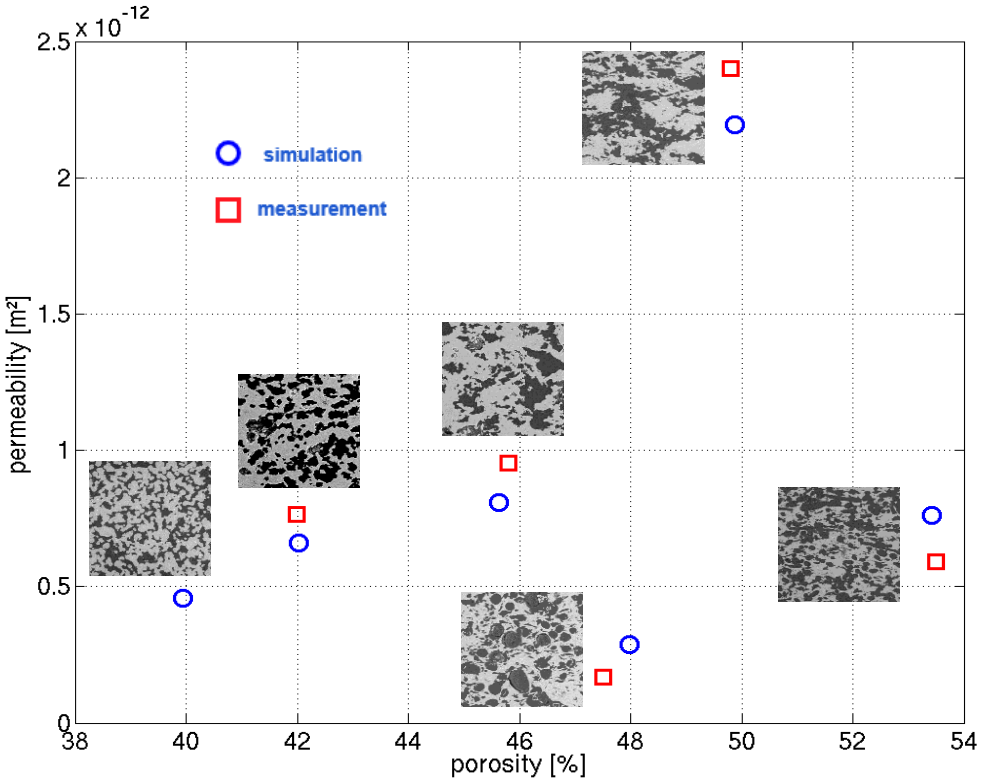

Figure 3: Measured porosities and permeabilities of real ceramics compared with modeled porosities and simulated permeabilities on modeled ceramics [7]

The micro-structure of sintered ceramic wall as shown on the left side of Figure 4 was generated with the GrainGeo Module of GeoDict. The size of the constructed geometry was 256 x 256 x 630 voxels in x, y, and z directions, with voxel length size of 0.9 µm. After generation of the micro-structure of the media, geometrical analysis was performed on the structure using the PoroDict module of GeoDict. As two illustrating examples in this study, the percolation path and the pore size distribution were computed and presented. The path of the largest particle which can pass through the media, known as percolation path, was visualized on the right side of Figure 4. The maximum particle diameter size which can pass through was found to be 9.94 µm and its corresponding path length was found to be 929 µm. The pore size distribution of the media was also computed and shown in Figure 5, once as cumulative distribution and once as fractional distribution.

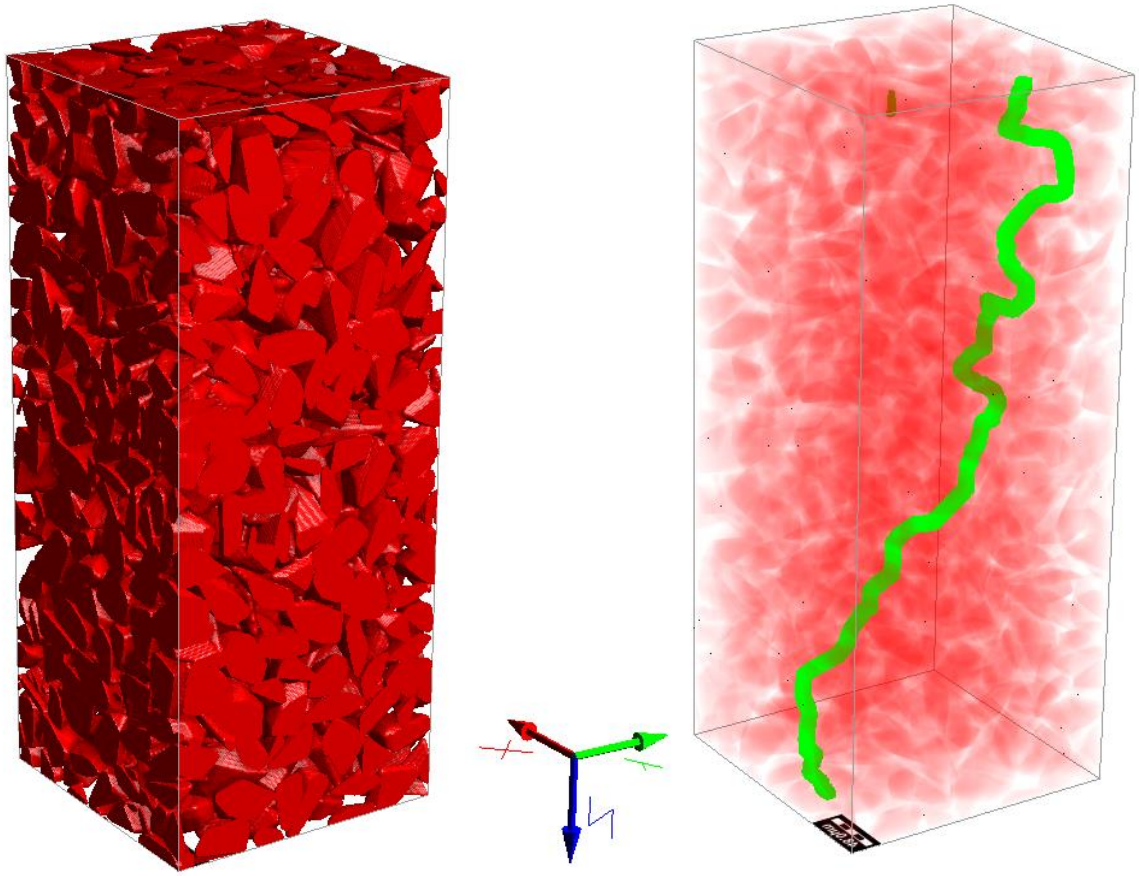

Figure 4: (left) micro-structure of sintered ceramic, (right) percolation path of the largest particle

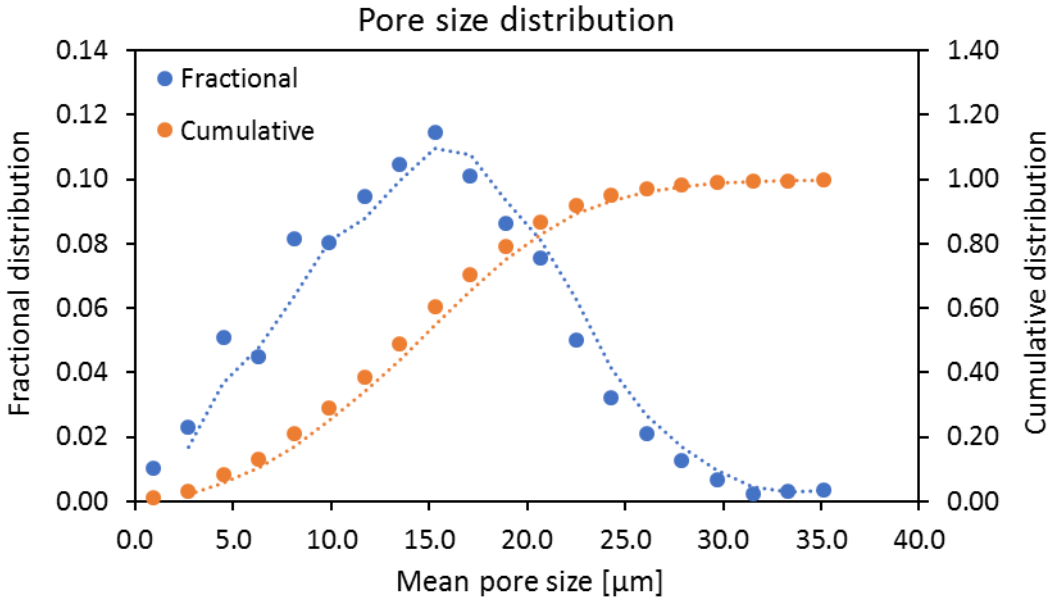

Figure 5: Characterization of pore size distribution with PoroDict module of GeoDict

3. Air flow simulation

The Navier-Stokes-Brinkman equations (1) are used in the filtration simulations to compute the fluid flow. In the filtration context, they were introduced by Iliev and Laptev [6]. Due to the creeping flow through the media, the equations are usually simplified to

the Stokes equations by dropping the nonlinear (inertia) term. On the media scale the Brinkman term is active in cells where soot has deposited. On the honeycomb scale, the Brinkman term is active in cells representing the walls and gets modified where soot deposits through the wall or on top of the wall.

$$\begin{aligned} \mu\Delta\vec{u} - \rho(\vec{u}\cdot\nabla)\vec{u} - \mu\kappa^{-1}\vec{u} &= \nabla p \text{ on } \Omega \quad (\text{Conservation of momentum}) \\ \nabla\cdot\vec{u} &= 0 \text{ on } \Omega \quad (\text{Conservation of mass}) \\ \vec{u} &= 0 \text{ on } \Gamma \quad (\text{No}-\text{slip on solid surfaces}) \end{aligned} \tag{1}$$

where

$\Omega \subset [0,\ l_x] \times [0,\ l_y] \times [0,\ l_z]$ (Domain)
$\vec{u}$: velocity vector
p: pressure
μ: dynamic viscosity
Γ: solid surface
ρ: density,
κ: porous voxel permeability.

4. Soot transport simulation

The particle motion is modeled by a Lagrangian approach. Eqn. (2) gives the precise formulation for the particle transport without collisions in the most general form. As the soot particles are tracked with the air, two terms contribute to the particle velocity. The radius and density (as mass) enter the friction of the particle against the flow, and also into the diffusive part of the motion.

$$m\frac{d\vec{v}}{dt} = 6\pi\mu\frac{R}{C_c}\left(\vec{u} - \vec{v} + \sqrt{2D}\frac{d\vec{W}(t)}{dt}\right) + Q\vec{E} \tag{2}$$

where

$\vec{v}$	: particle velocity [m/s]	μ	: dynamic viscosity [kg/m·s]
$\vec{u}$	: fluid velocity [m/s]	Q	: particle charge [C]
R	: particle radius [m]	E	: electric field [V/m]
C_c	: Cunningham correction	D	: Diffusivity [m²/s]
m	: particle mass [kg]	$d\vec{W}$	: 3D Wiener process

Electrostatic charges are in principle possible to be considered in the simulations, but were not activated here. Particles can be positioned anywhere in space, while the fluid velocity is only available at a discrete set of points in space, for example on cell walls in case of one particular finite difference solver. To approximate fluid velocities at all particle locations, these discrete velocity values are linearly interpolated.

5. Soot particle deposition and conversion to porous media

The flow and collision models account for mechanism of filtration, except for the influence of their mass and electrical charges, particles follow the streamlines and can be caught by direct interception. Due to their mass, they can leave streamlines and can be caught by inertial impact. For small particles, as it is the case for soot particles,

the effect of Brownian motion is significant, and they can be caught by diffusive deposition.

Because the particles are spherical, only the distance of the particle center from the nearest obstacle needs to be computed in order to detect collisions. To further accelerate this computation, the media model is equipped with a so-called distance function, which provides information about the distance to the nearest obstacle voxel for all empty voxels. If the particle radius is smaller than the distance function value at its position, then no collision can occur. In case of soot, the other situation is rather simple – the soot is assumed to be completely sticky, i.e. soot deposits on its first contact. Two cases must be distinguished. When the computational grid for the flow simulations resolves the particles, particle deposition simply turns previously empty grid cells into solid grid cells. More interestingly, when the grid does not resolve the particles, a depositing particle adds mass to the cell and the cell becomes porous. Two parameters must be determined for the simulation, the maximum achievable density and corresponding flow resistivity in this unresolved setting.

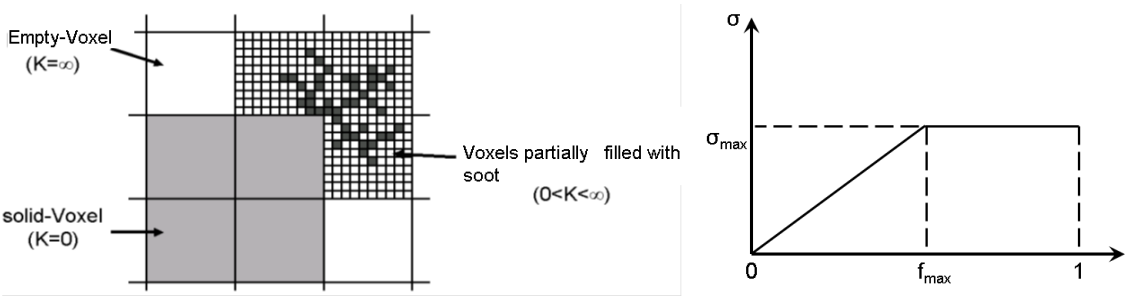

Figure 6: Soot deposited voxels are considered porous (left). The resistivity of the voxels depends linearly on the solid volume fraction (right).

In general, for porous media with low porosity, it is a standard assumption that flow resistivity depends linearly on the solid volume fraction. In our model, this linear relation is assumed up to a maximum packing density f_{max}, beyond which no more soot particles can enter a computational grid cell. Thus, the two independent parameters of the model are the maximal packing density of a cell and the flow resistivity of the cell at this packing density. In the graph on the right side of Figure 6, the packing density and flow resistivity correspond to the end point of the diagonal line and the slope of this line, respectively. Since numerically also packing densities slightly larger than f_{max} may occur, it is assumed that the resistivity σ_{max} does not increase when $f > f_{max}$, but remains as a constant.

$$k = \frac{\mu}{\sigma}, \qquad \sigma = \begin{cases} \frac{f}{f_{max}}\sigma_{max}, & 0 < f < f_{max} \\ \sigma_{max}, & f \geq f_{max} \end{cases}$$

Since the Navier-Stokes Brinkman equations are written in terms of the permeability κ, the relation of permeability and resistivity is also spelled out. Cheng et al. [1] described how the packing density and flow resistivity are determined in the multivariate

permeability model. In the new multivariate permeability model, σ_{max} is different for depth filtration, denoted by σ^1_{max}, and cake filtration denoted by σ^2_{max}.

6. Lifetime filtration simulation for ceramic structure

Figure. 7 shows the experimental data to which f_{max} and σ_{max} can be fitted. Two phases, depth and cake filtration can be clearly distinguished, and make it seem reasonable that different sets of parameters may be needed for the two phases. 3 parameters can be extracted: the slopes of the pressure drop over time in depth and cake filtration, s1 and s2, and the moment in time / amount of soot x for which the behavior changes from depth to cake filtration. As a closing assumption, we assume f_{max} to be the same for both phases, and are left with the need to fit $f_{max,}$ σ^1_{max} and $\sigma^2_{max.}$ This assumption is partially based on the fact that the experimental pressure drop curves, when scaled by the fluid velocity, all agreed to be on a master curve – at least for the relatively low mass flow rates under consideration. We concluded that the soot packing density has to be independent of the flow velocity, and should be the same in the pores of the ceramic as in the soot filter cake on top of the ceramic.

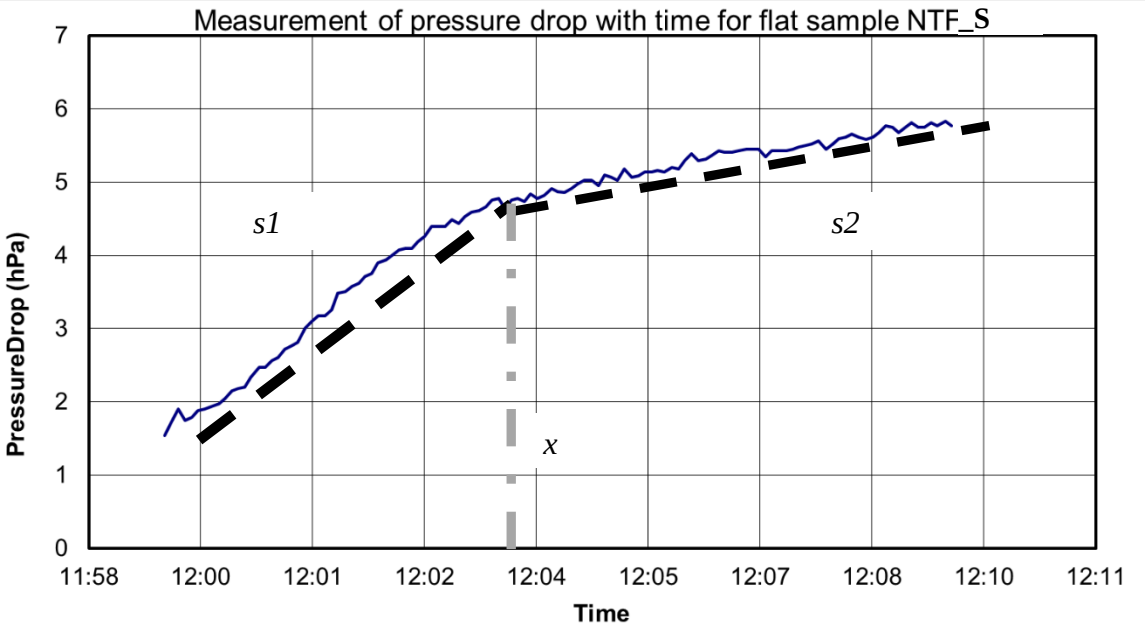

Figure. 7: Evolution of the pressure drop over time, as soot is depositing on the flat NTF_S sample.

Figure 8 shows the pressure drop evolution for 5 experiments and for 5 simulation runs, i.e. 5 different realizations of the ceramic model. The error bars on the simulation data are narrower than for the experimental data. This indicates that the small cutouts of the ceramic considered in the simulation are more homogeneous than the true ceramic – a typical phenomenon observed in several of our material simulation projects.

The parameters that were obtained by fitting the NTF_S sample were used to predict the behavior of NTF_B, a similar ceramic made from larger grains that result also in larger pores. Figure 9 shows the results of this prediction. Comparisons to multiple

experimental pressure drop curves show that these parameters predict extremely well the pressure drop of another DPF media. This work confirms an important step in virtual material design – the behavior of not-yet-existing materials can be predicted by computer simulations, as long as the parameters are established and validated against measurements of media that are not too different from the new and virtual ones. Depth filtration regime through the micro-structure of the ceramic wall and cake filtration regime above the media structure are visualized in Figure 10. Through plane z is the particulate flow direction which is shown on y axis of the diagram. Deposited volume of particles in $(\mu m)^3$ is shown on x axis of the diagram. The two red lines depicted inside this figure are supposed to be the bottom and top surfaces of the ceramic wall.

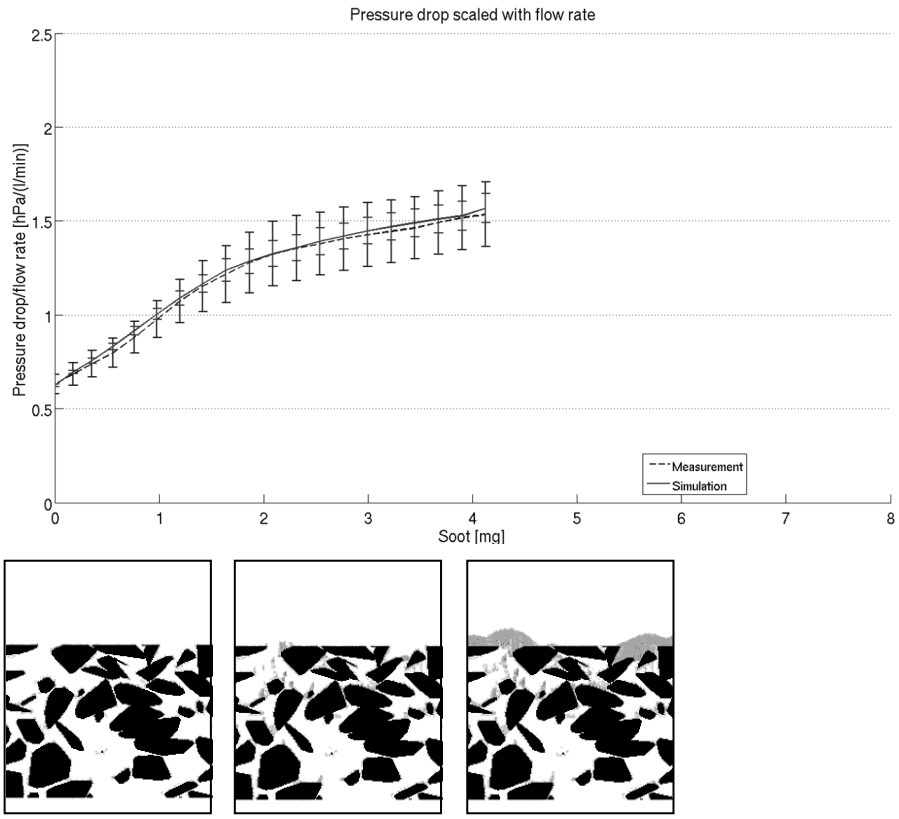

Figure 8: Experimental and simulated pressure drop evolution with error bars induced by 5 measurements and 5 different realizations of the virtual structure.

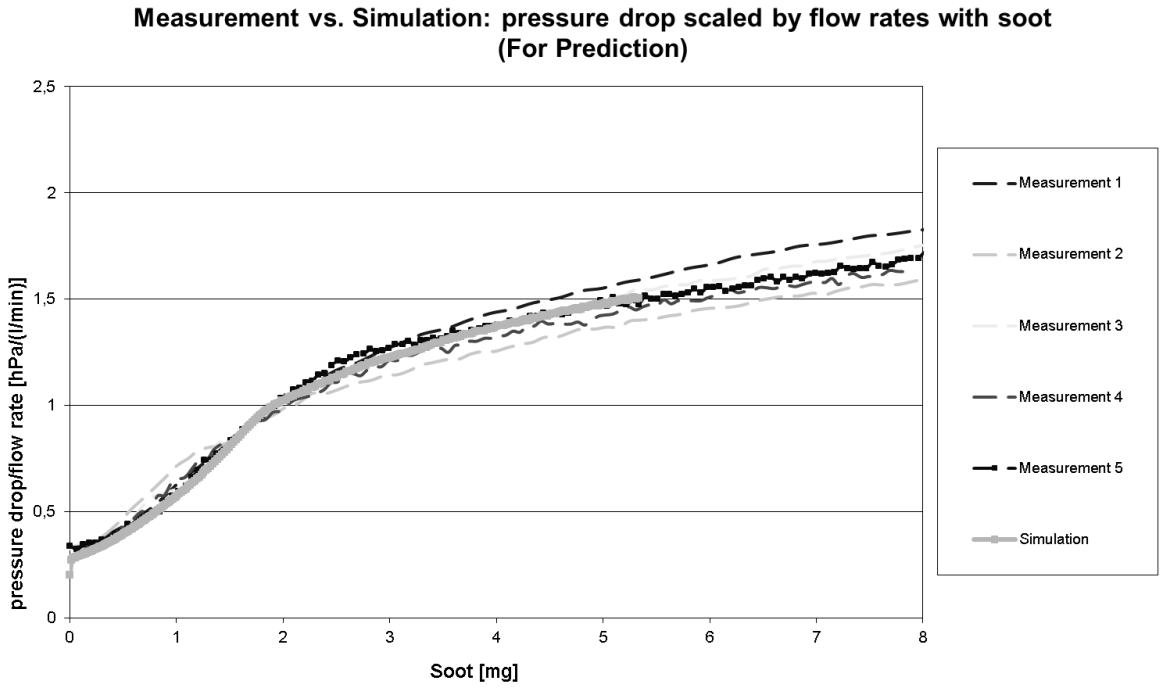

Figure 9: Experimental and simulated pressure drop for a different ceramic, with parameters found by fitting against the measurements in Figure 8.

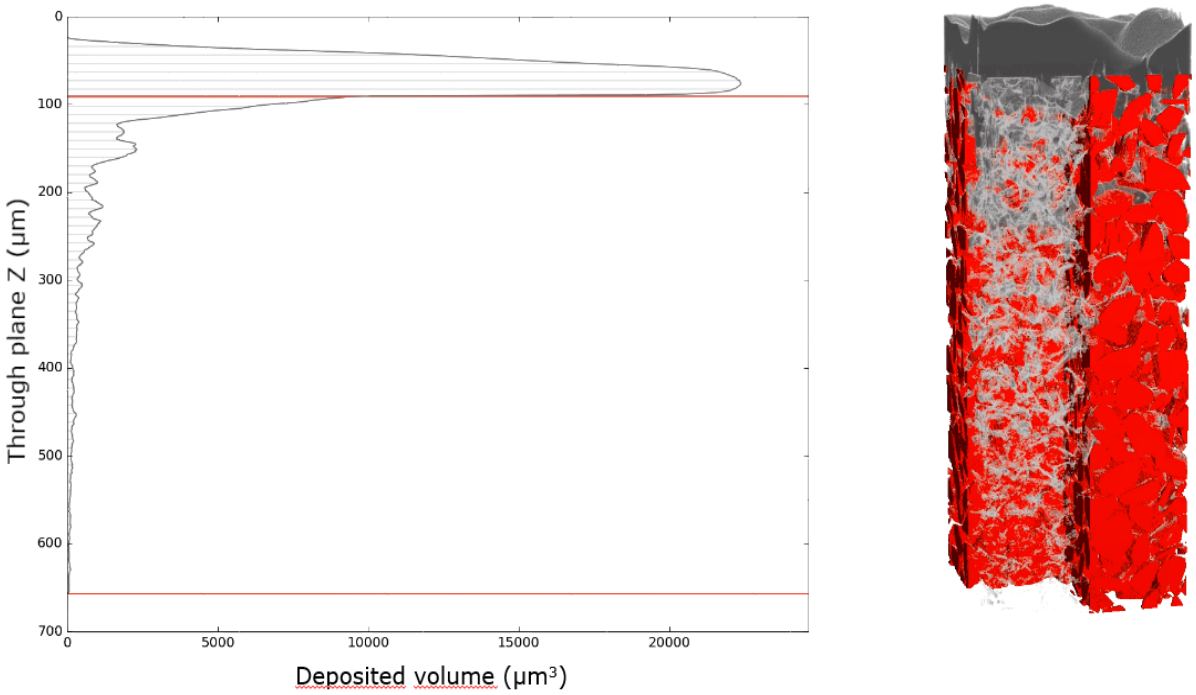

Figure 10: Soot particles deposition as depth and filter cake regimes

7. Filter life-time simulation on honeycomb structure

The behavior of the complete filter is what really matters in practice and not just the filter media. After obtaining ceramic properties, such as permeability and filter efficiency, it is possible to simulate the DPF filter on the next scale (Figure 11). To evaluate the performance of a DPF filter, the honeycomb structure can be studied taking many of the filter designs into account, such as channel shape, channel length, channel dimensions, wall thickness, plug behavior, etc.

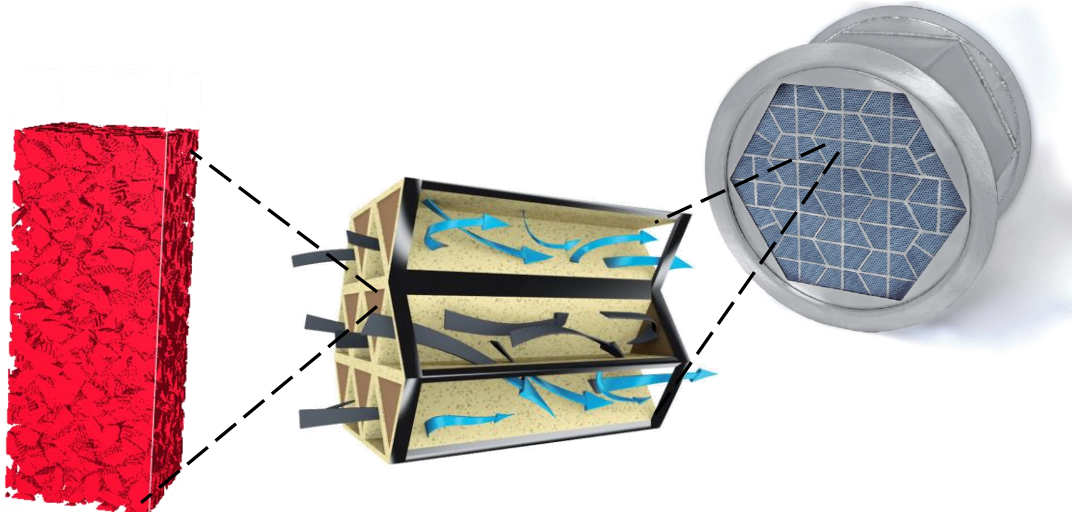

Figure 11. The multi-scale structure of DPF filter: the micro-scale, honeycomb structure, and DPF element.

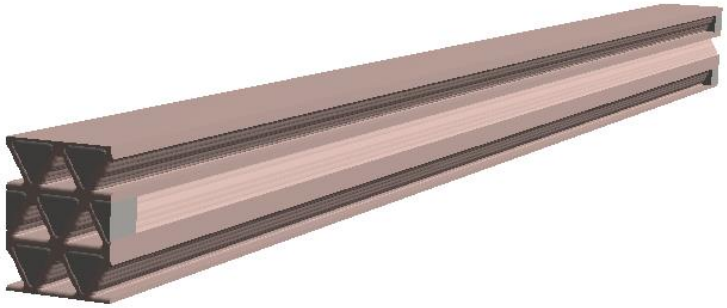

Figure 12. Honeycomb structure created by GeoDict

The honeycomb structure can be generated with GeoDict, by definition of shape and size of the channel, the thickness of the filter wall and plug (Figure 12). The same equations as for the micro-scale, describe the air flow and the particle motion. Now, the ceramic must be modeled as porous media with density and permeability, and these may change as particles are deposited. A complex interplay of soot cake growth and channel diameter reduction add to the pressure drop in a way not considered for flat samples, and the sheer number of soot particles to be handled by the simulation grows from hundreds of millions on the media scale to hundreds of billions on the honeycomb scale. Figure 13 shows flow streamlines through a honeycomb structure, and the soot particles collected inside the filter media as well as on the surface.

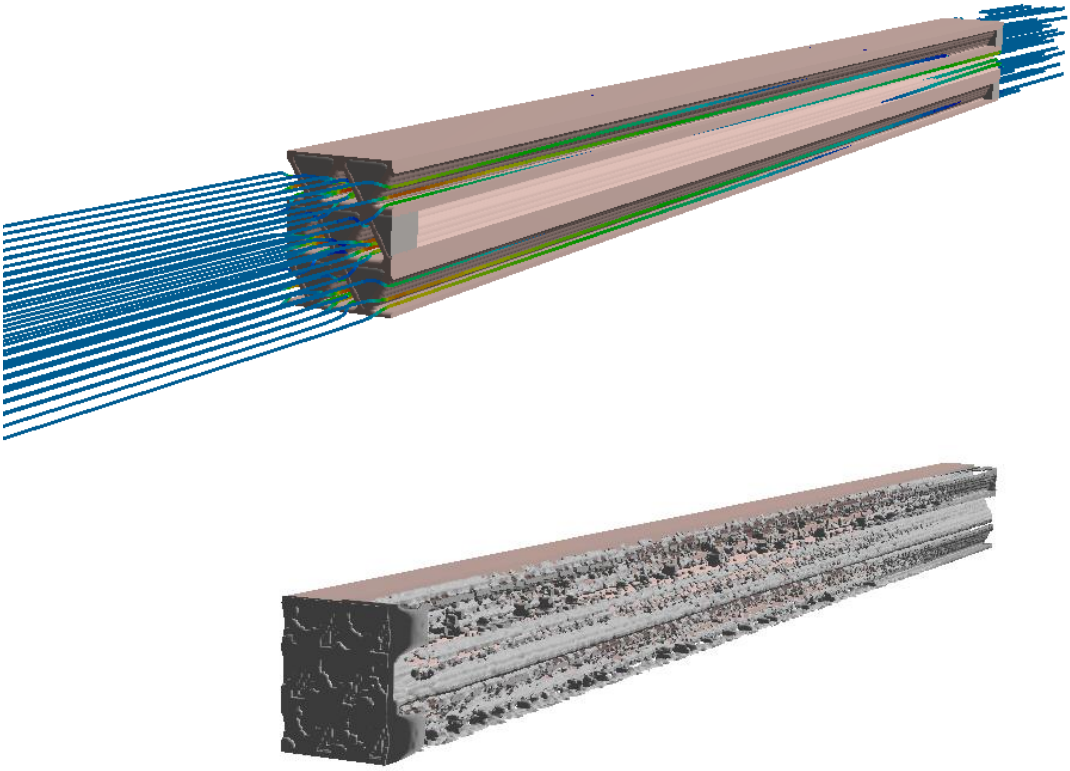

Figure 13. The streamlines of the flow in a honeycomb structure (top) and soot collected inside the filter media and on the ceramic surfaces (bottom)

8. Conclusions

The ceramic material and filter design can be done with the Digital Material Laboratory, GeoDict software package for DPF. In the micro-scale, 3D ceramic structures can be modeled and the properties of the filter material can be predicted with the soot filtration life-time simulations. In the honeycomb scale, honeycomb structures can be created in minutes. The pressure drop evolution and soot loading can be simulated to know the performance of the filter. The parameters found by matching the measurements on one medium can be used to predict a new not-yet-existing medium, which makes the digital design possible. The project to simulate soot filtration in DPF resulted in an improved DPF and a patent was granted.

References

[1] L. Cheng, S. Rief, A. Wiegmann, J. Adler, L. Mammitzsch and U. Petasch, Simulation of Soot Filtration on the Nano-, Micro- and Meso-scale, Proceedings of 11th World Filtration Congress, 17.-19. April 2012, Graz, Austria.

[2] J. Adler and U. Petasch, Effect of membranes in exhaust particulate filtration. Advances in Ceramic Armor, Bioceramics, and Porous Materials, Ceramic

Engineering and Science Proceedings Vol. 37 (4), Ed. Jerry C. LaSalvia, Ed. Roger Narayan, Ed. Paolo Colombo, John Wiley & Sons, 2016, pp. 139-147.

[3] Patent No. DE102012220181 A1, http://www.google.com/patents/DE102012220181A1?cl=en

[4] Ohser, J., Mücklich, F.: “Statistical Analysis of Microstructures in Materials Science”, John Wiley & Sons, 2000.

[5] J. Becker, E. Glatt, A. Wiegmann, GeoDict, http://www.geodict.com, 2018.

[6] O. Iliev, V. Laptev. On Numerical Simulation of Flow through Oil Filters, J. Computers and Visualization in Science, vol. 6, 2004.pp. 139-146.

[7] K. Schmidt and J. Becker, Generating Validated 3D Models of Microporous Ceramics, Adv. Engineering Materials, Volume 15, Issue 1-2, pp 40-24, 2013.